Impact of numerical models on fragmentation processes

Mathieu Renouf, Belien Gezahengn, Micheline Abbas, Florent Bourgeois

Impact of Numerical Models on Fragmentation Processes

Mathieu Renouf*, Belien Gezahengn*, Micheline Abbas† and Florent Bourgeois†

*LMGC, CNRS-UM2, UMR 5508, Montpellier, France
†LGC, CNRS, UMR, Toulouse France

Abstract. Simulated fragmentation process in granular assemblies is a challenging problem which date back the beginning of the 90'. If first approaches have focus on the fragmentation on a single particle, with the development of robust, fast numerical method is is possible today to simulated such process in a large collection of particles. But the question of the fragmentation problem is still open: should the fragmentation be done dynamically (one particle becoming two fragments) and according which criterion or should the fragment paths be defined initially and which is the impact of the discretization and the model of fragments? The present contribution proposes to investigate the second aspect i.e. the impact of fragment modeling on the fragmentation processes. First to perform such an analysis, the geometry of fragments (disks/sphere or polygon/polyhedra), their behavior (rigid/deformable) and the law governing their interactions are investigated. Then such model will be used in a grinding application where the evolution of fragments and impact on the behavior of the whole packing are investigate.

Keywords: DEM, Fragmentation, CZM
PACS: 45.70.Mg,45.70.-n,62.20.mm

INTRODUCTION

Simulated fragmentation process in granular assemblies is a challenging problem which date back the beginning of the 90'. First approaches have focus on the fragmentation on a single particle and the different parameters of interaction law [1, 2] or on the fragmentation algorithm [3]. The works have been extended to the simulation of the fragmentation of a collection of particles under compression [4] and to the combining of rigid and deformable particles [5]. More recently, such methods are compared to experimental process [6], proposing good agreements and could be applied on grinding simulation process [7]. But the question of the fragmentation problem is still open: should the fragmentation be done dynamically (one particle becoming two fragments) and according which criterion or should the fragment paths be defined initially and which is the impact of the discretization and the model of fragments?

The present contribution proposes to investigate the second aspect i.e. the impact of fragment modeling on the fragmentation processes. First to perform such an analysis, the geometry of fragments (disks or polygon) and the law governing their interactions are investigated. Numerical results are compared to experimental ones, resulting from the impact of steel sphere on a pyrex bead lying on a impact bar. Then such model will be used in a grinding application where the evolution of fragments and impact on the behavior of the whole packing are investigate.

NUMERICAL STRATEGY

To simulate our collection of particles, the Non Smooth Contact Dynamics method (NSCD) developed by Moreau [8] and Jean [9] is used. The headlines of the original approach are the following. Let's consider the equation of motion using to describe the evolution of a collection of rigid bodies:

$$\mathbb{M}\ddot{q} = \mathbf{F}^{ext} + \mathbf{R}, \tag{1}$$

where $\mathbb{M}$ denotes the mass matrix, $\ddot{\mathbf{q}}$ the second time derivative of configuration parameter $\mathbf{q}$. The forces of the system are decomposed into external forces $\mathbf{F}^{ext}$ and the resultant of contact forces $\mathbf{R}$. The equation (1) is rewritten in a framework which allow the derivation of acceleration when shock are expected using a θ-method, where θ is equal to 0.5 for stability reason ad to keep a conservative time scheme.
Thus, over the time interval $[t_i, t_{i+1}]$, of measure h, one obtain the following system:

$$\left\{ \begin{array}{l} \mathbf{q}_{i+1} = \mathbf{q}_i + \theta \dot{\mathbf{q}}_{i+1} + (1-\theta)\dot{\mathbf{q}}_i \\ \dot{\mathbf{q}}_{i+1} = \dot{\mathbf{q}}_{i+1}^{free} + \mathbb{M}^{-1} h \mathbf{R}_{i+1} \end{array} \right. , \tag{2}$$

with

$$\dot{\mathbf{q}}_{i+1}^{free} = \dot{\mathbf{q}}_i + h\mathbb{M}^{-1}(\theta \mathbf{F}_{i+1}^{ext} + (1-\theta)\mathbf{F}_i^{ext}). \tag{3}$$

The resolution of system (2) is performed by looking for the unknowns $(h\mathbf{R}_{i+1}, \dot{\mathbf{q}}_{i+1})$ related to the elements of the system. To the research of such couple of unknowns, one prefers looking for its dual $(\mathbf{r}_{i+1}, \mathbf{u}_{i+1})$ composed of the local contact impulsion and the contact relative velocity,

related to $(h\mathbf{R}_{i+1}, \dot{\mathbf{q}}_{i+1})$ via the linear mappings $\mathbb{H}$ et $\mathbb{H}^*$:

$$\left\{ \begin{array}{rcl} h\mathbf{R} & = & \mathbb{H}\mathbf{r} \\ \mathbf{u} & = & \mathbb{H}^*\dot{\mathbf{q}} \end{array} \right. . \tag{4}$$

By introducing the equations of system (4) in system (2), one obtains:

$$\left\{ \begin{array}{l} \mathbb{W}\mathbf{p}_{i+1} + \mathbf{u}_{i+1} = \mathbb{M}^{-1}(h(1-\theta)\mathbf{F}_i^{ext} + h\theta\mathbf{F}_{i+1}^{ext}) \\ Interaction[\mathbf{r}_{i+1}, \mathbf{u}_{i+1}] \end{array} \right. , \tag{5}$$

where $\mathbb{W}(= \mathbb{H}^*\mathbb{M}^{-1}\mathbb{H})$ represents the Delassus operator and $Interaction[\mathbf{r}_{i+1}, \mathbf{u}_{i+1}]$, the interaction law relating contact impulsions and contact relative velocities. The algorithm used to solve the contact problem is a Non-Linear Gauss-Seidel algorithm, looking for a solution by a contact-wise treatment. The reader could refers to original works for more information [9, 8].

To close the system (5), the interaction law which relate $\mathbf{r}$ and $\mathbf{u}$ should be defined. The present model, used to describe the interaction between particles has been proposed by Raous et al [10] and is based on five parameters: C_n and C_t the normal and tangential stiffness respectively; w, the de-cohesion energy; b, the viscosity associated to the evolution of the adhesion and μ the local friction coefficient. The intensity of the adhesion of the interaction is characterized in this model by the internal variable β, introduced by Frémond [11]. It takes its values between 0 and 1 (0 is no adhesion and 1 is perfect adhesion). The use of a damageable stiffness of the interface, depending on β, ensures a good continuity between contact conditions during the process:

$$\frac{\partial \beta}{\partial t} = -\frac{1}{b}(w - \beta(C_n u_n^2 + C_t u_t^2))^-, \tag{6}$$

where q^- denotes the negative part of the quantity q. For the purposes of the present work, no viscosity between particles is considered ($b = 0$). Initially interactions are perfectly intact (β=1) and normal and tangential stiffness are considered equal. This means that the local model is defined through three parameters, i.e. C_n, μ and w.

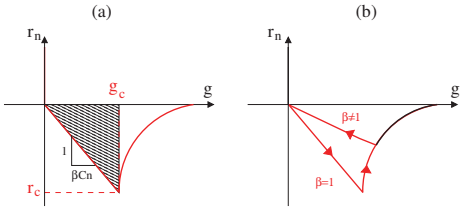

FIGURE 1. Cohesive Zone Model force profile ; (a) elastic range definition and (b) beta value.

Fig. 1 proposes an illustration of a typical CZM graph. The maximal traction force r_c is equal to $\sqrt{wC_n}$ while the corresponding distance defining the elastic range (without damage), g_c, is equal to $\sqrt{w/C_n}$. Note that when such law is used in discrete element assemblies, it is necessary to take care during the contact detection process. Indeed, to avoid overlap between particles, an alert distance is used to anticipate a potential contact. Usually, this distance should not be too large to minimize the number of contact (active or not). With the presence of CZM, the alert distance should not be too small to cut the CZM graph and dissipate energy numerically.

EXPERIMENTAL SET-UP

To support our numerical results, an experimental set-up based on a Hopkinson bar is used (c.f. Fig.2). The experiment consist in the impact of a steel sphere on a pyrex bead lying on a impact bar.

FIGURE 2. Visualization of the experimental set-up based on a Hopkinson bar

The diameter of the pyrex bead is equal to 6 *mm* with a density ρ equal to 2 230 $kg.m^{-3}$. The steel sphere diameter is equal to 60 *mm* with a density equal to 7 600$kg.m^{-3}$. The initial distance between the steel sphere and the plan is equal to 80 *mm*. No initial velocity is given to the sphere. The experiment is performed on a set of 30 pyrex beads. The force resulting of the impact of the sphere on the bar is measured and plotted on Fig.3

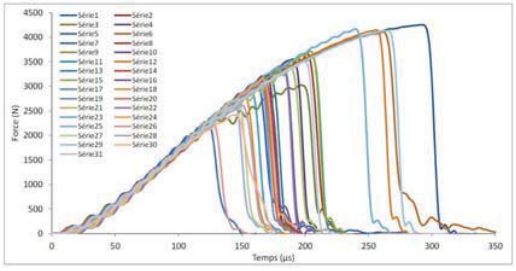

FIGURE 3. Evolution of the force measured on the impact bar for the whole bead set.

All Profiles respect approximatively the same evolution. The bifurcation point (force threshold) on the evo-

lution of the force corresponds to the fragmentation of the particle during its loading. The force threshold is distributed along the loading curve. This distribution is dependent of the initial position of the particles on the bar and reflects the real heterogeneity of brittle properties of pyrex particles.

NUMERICAL RESULTS

On a single particle

First of all, simulation have been performed on a single particles. Different meshes have been used to discretize the single particle: meshes composed of 2 940 and 11 689 disks and meshes composed of 954 (c) and 6 754 (d) polygons (c.f. Fig. 4).

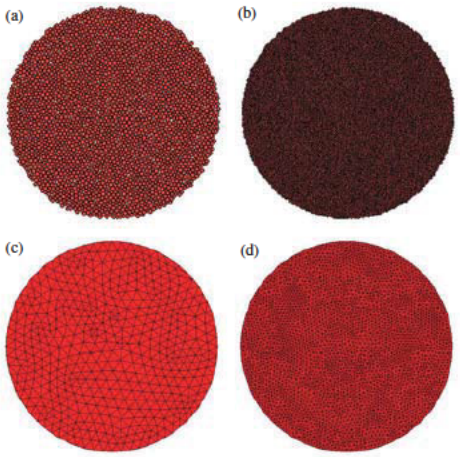

FIGURE 4. Samples used in the different simulations : meshes composed of 2 940 (a) and 11 689 (b) disks and meshes composed of 954 (c) and 6 754 (d) polygons

As discrete elements are used as a meshless method, influence of the discretization have been tested and 10 samples composed of 2 940 disks have been created. Then the damage of the macro-particle (as the number of broken links) and the impact force on the impact bar are measured for different values of the maximal traction force C_n as well as the friction coefficient μ between disks.

Logically, the increase of the value of C_n reduces the number of broken links in the macro-particle (c.f. Fig. 5). Such process is independent of the discretization (small amplitude of the error bars).

In parallel, the impact force is measured (c.f. Fig. 6). Larger is the local maximal traction force, larger the measured force is. For a too large value, the particle is strong enough to repulse the impact bar. Consequently, the smaller value of C_n is used to analyze the influence of μ.

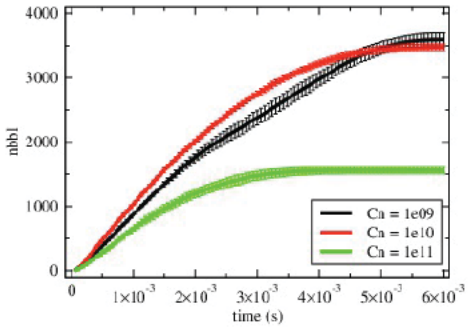

FIGURE 5. Evolution of the mean damage evolution for three value of C_n and fixed values for μ and w (resp. equal to 0.1 and 5 10^{-2})

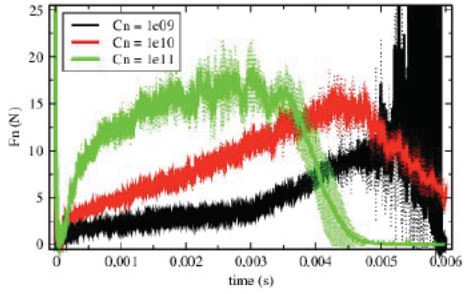

FIGURE 6. Evolution of the mean impact force evolution for three value of C_n and fixed values for μ and w (resp. equal to 0.1 and 5 10^{-2})

The increase of μ increases the number of broken links within the macro-particles and reduced the variation due to the discretization (c.f. Fig. 7).

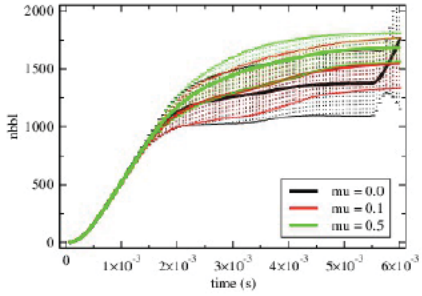

FIGURE 7. Evolution of the mean damage evolution for three value of μ and fixed values for C_n and w (resp. equal to 10^9 and 5 10^{-2})

The increase of μ does not affect the first part of the evolution of the impact force (c.f. Fig. 8). Then for a large value of μ, the impact force decreases slowly. This is due

to the presence of large fragment in the contact which are broken by the impact bar.

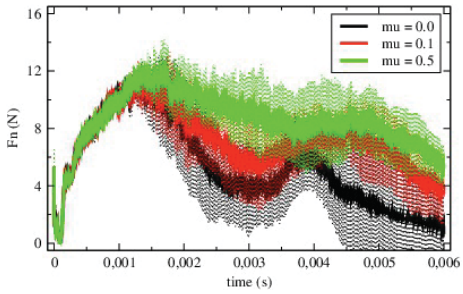

FIGURE 8. Evolution of the mean impact force evolution for three value of μ and fixed values for C_n and w (resp. equal to 10^9 and 5 10^{-2})

The increase of μ does not affect the first part of the evolution of the impact force (c.f. Fig. 8). Then for a large value of μ, the impact force decreases slowly. This is due to the presence of large fragment in the contact which are broken by the impact bar.

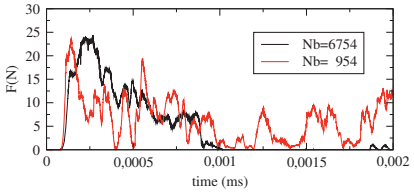

FIGURE 9. Evolution of the mean impact force evolution for sample (c) and (d) for a triplet (C_n, μ, w) equal to $(10^9, 0.1, 5\ 10^{-2})$

Finally, the influence of polygon mesh is analyzed (c.f. Fig. 9). One could observed that the impact force value is independent of the mesh. This value is larger for a collection of polygons (˜25N) that for a collection of disks (˜12N). This is could be explain by the fact that is more difficult for a polygon to move than a disk. Such behavior plays also an important role in the decrease of the curve which is faster for polygons

On a collection of particles

Such modeling could be applied on a collection of particles where each particle is a collection of polygons (100 particles composed of 54 elements, c.f. Fig. 10). The fragmentation process is observed during the rotation of the drum.

The initial drop-off of particles create a small evolution of the global damage. Then when particles start to flow at the free surface, the global damage increase linearly to reach a steady state where fragments created during the process preserve the damage of undamaged particles.

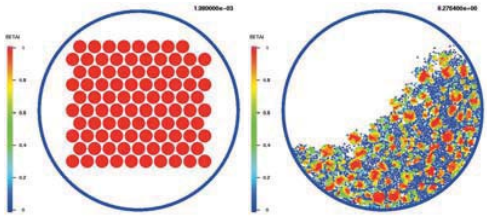

FIGURE 10. Fragmentation of particles in a rotating drum

CONCLUSION

To conclude, a comparison with experimental result, underlined the weakness of rigid modeling for such process. Indeed, there is some elasticity in compression. This elasticity measured is related to contact, orthogonal to the loading direction, which are working in traction. Improvement in terms local contact law as well as element deformation could be performed.

Acknowledgment This work is supported by the ANR project FReIN.

REFERENCES

1. A. Potapov, and C. Campbell, *Powder Technol.* **81**, 207–216 (1994).
2. F. Kun, and H. Herrmann, *Comput. Meth. Appl. Mech. Engrg* **138**, 3–18 (1996).
3. G. Hernandez, and H. Herrmann, *Phys. A* **215**, 420–430 (1995).
4. A. Potapov, and C. Campbell, *Powder Technol.* **94**, 109–122 (1997).
5. A. Munjiza, and N. John, *Eng. Fract. Mech.* **69**, 281–295 (2002).
6. Y. Wang, and F. Tonon, *Int. J. Rock Mech. Mining Sci.* **48**, 535–545 (2011).
7. J. Bruchm uller, B. van Wachem, S. Gua, and K. Luo, *Powder Technol.* **208**, 731–739 (2011).
8. J. J. Moreau, "Unilateral contact and dry friction in finite freedom dynamics," in *Non Smooth Mechanics and Applications, CISM Courses and Lectures*, edited by J. Moreau, and e. P.-D. Panagiotopoulos, 1988, vol. 302 (Springer-Verlag, Wien, New York), pp. 1–82.
9. M. Jean, *Compt. Methods Appl. Math. Engrg.* **177**, 235–257 (1999).
10. M. Raous, M. Cangémi, and M. Cocu, *Comput. Methods Appl. Mech. Engrg.* **177**, 383–399 (1999).
11. M. Frémond, *J. Mec. Theor. Appl.* **6**, 383–407 (1987).